

# Convexity and Robustness of Dynamic Traffic Assignment for Control of Freeway Networks

Giacomo Como \*    Enrico Lovisari    Ketan Savla

June 5, 2022

## Abstract

We study System Optimum Dynamic Traffic Assignment (SO-DTA) for realistic traffic dynamics controlled by variable speed limits, ramp metering, and routing controls. We consider continuous-time cell-based Dynamic Network Loading models that include as special cases the Cell Transmission Model (CTM) with FIFO rule at the diverge junctions as well as non-FIFO diverge rules. While a straightforward consideration of traffic dynamics and control variables in the SO-DTA is known to lead to a non-convex program, and hence is computationally expensive for real-time applications, we consider SO-DTA formulations in which the total inflow into and the total outflow from the cells are independently constrained to be upper bounded by concave supply and demand functions, respectively, thus preserving convexity. We then design open-loop controllers that guarantee that the optimal solutions under the relaxed constraints are feasible with respect to realistic traffic dynamics. We develop this methodology for three variations of the SO-DTA problem that impose constraints on turning ratios to varying degrees. Using tools from optimal control, we identify specific scenarios in which the optimal solution under the relaxed constraints is readily feasible with respect to the CTM, and hence no additional control is needed. We also evaluate the robustness of the system trajectory under the proposed controllers by deriving bounds on the deviations induced by perturbations of the initial condition and of the external inflows. Finally, shrinking of the feasible set for SO-DTA by scaling down of the supply functions is explored as a means to ensure free-flow operation even under perturbations in external inflow. The resulting tradeoff with nominal cost is illustrated via numerical simulations.

---

\*G. Como is with the Department of Automatic Control, Lund University, Sweden. [giacomo.como@control.lth.se](mailto:giacomo.como@control.lth.se). E. Lovisari was with Univ. J. Fourier and GIPSA-lab, CNRS, Grenoble, France. [enrico.lovisari@gipsa-lab.fr](mailto:enrico.lovisari@gipsa-lab.fr). K. Savla is with the Sonny Astani Department of Civil and Environmental Engineering at the University of Southern California, Los Angeles, CA. [ksavla@usc.edu](mailto:ksavla@usc.edu). The authors are listed in alphabetical order.

# 1 Introduction

Dynamic Traffic Assignment (DTA), introduced in [20, 21], has attracted a large amount of attention by the transportation research community, and has become a standard framework for control of freeway networks, see [23] for an overview. The focus of this paper is on System Optimum Dynamic Traffic Assignment (SO-DTA) that aims at minimizing a system-level cost function over a planning horizon, subject to realistic traffic dynamics, and the presence of variable speed limits, ramp metering, and routing control.

The Cell Transmission Model (CTM), originally proposed in [8], is a compelling framework to simulate realistic traffic dynamics. It consists of a space discretization of the kinematic wave models of [18] and [24]. The CTM allows for capturing fundamental traffic phenomena, such as disturbance propagation and creation of shockwaves on freeways, and can be adapted to account for traffic signal control and ramp metering devices. While standard CTM frameworks on networks [9] enforce the turning ratios (determined either exogenously or by a routing policy, e.g., in an evacuation scenario) under all circumstances by employing a First In First Out (FIFO) policy, recent work, e.g., see [10, 17], has also considered non-FIFO policies that allow for deviations from turning ratios to model the tendency of drivers to avoid congestion. Motivated by these variations, we model traffic dynamics using a combination of the cell-based feature of CTM and a general Dynamic Network Loading model [3] that includes both FIFO and non-FIFO policies.

Variable speed limits, ramp metering, and routing are the most widely studied forms of control for freeway networks. Examples of such studies include [12] and [6], which employ ramp metering to minimize travel time and maximize network throughput at equilibrium, respectively, [15] that uses variable speed limits to suppress shock-waves, and [4] that develops information routing strategy for evacuation. However, with very few exceptions, e.g., see [22], these control strategies have not been incorporated in DTA formulations. The primary reason for not incorporating realistic traffic dynamics and control strategies in DTA is that finding numerical solutions for the resulting optimization problem is in general computationally expensive, and hence unsuitable for real-time applications. For example, [22] notes that, modeling traffic dynamics by a link-node cell transmission model and incorporating variable speed limits and ramp metering variables directly into the DTA formulation leads to a non-convex program.

Convexity is a desirable property of optimization problems that facilitates their fast numerical solution, e.g., using readily available software tools such as `cvx` [7, 13]. In fact, there have been efforts to relax non-convex features of traffic dynamics and control variables in DTA. For example, for linear demand and affine supply functions in CTM, and linear cost, [26] shows that the SO-DTA problem for single destination networks with no control variables can be cast as a linear program under the relaxation where the total inflow into and the total outflow from the cells are independently constrained to be upper bounded by supply and demand, respectively. While the optimal solution to the relaxed problem obviously has no higher cost than the original formulation, it is not

clear if it is feasible with respect to some realistic traffic dynamics.

Interestingly, [22] shows that the optimal solution obtained under the same relaxation proposed in [26] can be realized exactly for traffic dynamics modeled by the link-node cell transmission model using ramp metering and variable speed limits, when demand functions are linear, supply functions are affine, and the network consists of a mainline with on- and off-ramps. The existing efforts to investigate the feasibility of optimal solutions under relaxed constraints for realistic traffic dynamics and control are very few and limited to specific types of demand and supply functions, network structure, and DNL model. Our primary objective in this paper is to extend the state-of-the-art substantially beyond these limited scenarios.

In this paper, we consider continuous-time version of cell-based models for traffic flow dynamics. The mass balance principle describes the dynamics of traffic volumes in each cell through an ordinary differential equation. This dynamics imposes linear constraints between mass and inter-cell flows. Similar to [26, 22], and as in standard CTM models, the total inflow in and the total outflow from every cell are upper bounded by its supply and its demand functions, respectively. These constraints, which are relaxations of realistic traffic dynamics, are convex, when both the demand and the supply functions are concave — which corresponds to the standard assumption that the fundamental diagram is concave (see Fig. 1).

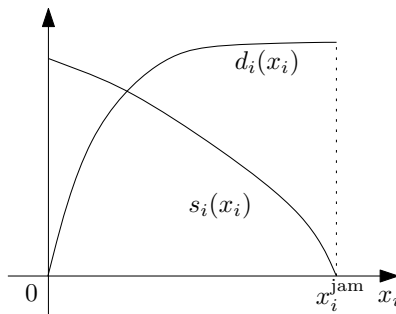


Figure 1: Example of concave demand ( $d_i(x_i)$ ) and supply ( $s_i(x_i)$ ) functions.

Therefore, these constraints, which do not prescribe turning ratios, combined with a convex cost imply convexity of the resulting SO-DTA formulation. This can already be considered as a generalization of [26]. Moreover, unlike [26], we also design (open-loop) variable speed, ramp metering and routing controllers under which the optimal solution of SO-DTA is exactly realizable under FIFO and non-FIFO DNL models.

When turning ratios are exogenously prescribed and cannot be controlled, e.g., as in [22], this feature can be incorporated in SO-DTA as linear equality constraints, thereby maintaining convexity. We also design open-loop variable speed and ramp metering controllers under which the optimal solution to this

constrained version of SO-DTA is exactly realizable under FIFO and non-FIFO DNL models. This methodology can be interpreted as generalization beyond the specific scenarios considered in [22]. Interestingly, we show that for networks consisting only of ordinary, merge, and diverge intersections, and whose cells have linear demand functions and affine supply functions with identical slopes, the optimal solution of the constrained SO-DTA with total traffic volume as cost is readily feasible with respect to the FIFO DNL model.

The secondary objective of this paper is to study robustness of optimal SO-DTA solutions with respect to uncertainties in initial condition and external inflow over the planning horizon. We provide bounds on the perturbation of the system trajectory under the proposed open-loop controllers in terms of perturbations in initial condition and external inflows. The system trajectory under the proposed controller is in free-flow, and hence it satisfies a certain monotonicity property. Our bounds, which leverage this monotonicity property, are applicable for relatively larger values of perturbations than those obtained through sensitivity analysis of ordinary differential equations. The proposed bounds are shown to be in close agreement with simulation results performed on the benchmark network in [26]. Finally, shrinking of the feasible set for SO-DTA by scaling down of the supply functions is explored as a means to ensure free-flow operation even under perturbations in external inflow. The resulting tradeoff with nominal cost is illustrated in simulations.

The paper is organized as follows. In Section 2, we present three variations of cell-based continuous-time SO-DTA that impose constraints on turning ratios to varying degrees. Section 3 presents open-loop variable speed, ramp metering, and routing controller under which the optimal solution to the three variations of SO-DTA are feasible with respect to traffic dynamics for general DNL models including FIFO and non-FIFO policies. This section also identifies scenarios under which no controller is required to have such feasibility. Section 4 presents perturbations bounds in optimal DTA solution due to perturbations in initial condition and external inflows. Finally, Section 5 draws conclusions and suggests future research directions. The proofs of the technical results are presented in the Appendix.

## 2 Convex Formulations for Continuous Time Dynamic Network Traffic Assignment

We describe the topology of the transportation network as a directed multi-graph  $\mathcal{G} = (\mathcal{V}, \mathcal{E})$  with nodes representing junctions and links  $i \in \mathcal{E}$  representing cells. The head and tail nodes of a cell  $i$  are denoted by  $\tau_i$  and  $\sigma_i$ , respectively, so that the cell is directed from  $\sigma_i$  to  $\tau_i$ . One particular node  $w \in \mathcal{V}$  represents the external world, with cells  $i$  such that  $\sigma_i = w$  representing on-ramps and cells  $i$  such that  $\tau_i = w$  representing off-ramps. The sets of on-ramps and off-ramps will be denoted by  $\mathcal{R}$  and  $\mathcal{R}^o$ , respectively. The network topology is typically illustrated by omitting such external node  $w$  and letting on-ramps have no tail

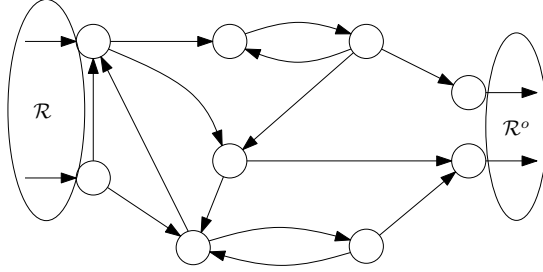


Figure 2: A multi-origin multi-destination cyclic network.

node and off-ramps have no head node. (See Figure 2.) We will use the notation

$$\mathcal{A} = \{(i, j) \in \mathcal{E} \times \mathcal{E} : \tau_i = \sigma_j \neq w\}$$

for the set of all pairs of adjacent (consecutive) cells.<sup>1</sup>

The dynamic state of the network is described by a time-varying vector  $x(t) \in \mathcal{R}^{\mathcal{E}}$  whose entries  $x_i(t)$  represent the mass (or traffic volume) in the cells  $i \in \mathcal{E}$  at time  $t$ . The inputs of the network are the inflows  $\lambda_i(t) \geq 0$  at the on-ramps  $i \in \mathcal{R}$ . Conventionally, we set  $\lambda_i(t) \equiv 0$  for all non on-ramp cells  $i \in \mathcal{E} \setminus \mathcal{R}$ , and stack up all the inflows in a vector  $\lambda(t) \in \mathcal{R}^{\mathcal{E}}$ . The physical constraints are captured by the demand functions  $d_i(x_i)$  and the supply functions  $s_i(x_i)$  (see Fig. 1), returning the maximum possible outflow from cells  $i \in \mathcal{E}$  and the maximum possible inflow in the non on-ramp cells  $i \in \mathcal{E} \setminus \mathcal{R}$ , respectively, as a function of the current mass  $x_i$ . Conventionally, we put  $s_i(x_i) \equiv +\infty$  at all on-ramps  $i \in \mathcal{R}$ . The demand functions are assumed to be continuous, non-decreasing, and such that  $d_i(0) = 0$ , while the supply functions are assumed to be continuous, non-increasing, and such that  $s_i(0) > 0$ , with  $x_i^{\text{jam}} = \inf\{x_i > 0 : s_i(x_i) = 0\}$  denoting cell  $i$ 's jam mass. Throughout, we focus on the case where all demand and supply functions are concave in their argument, which includes the common case of piecewise affine functions.

When formulating the DTA problems we will assume to be given an initial value  $x_i^0 \geq 0$  on every cell  $i \in \mathcal{E}$  and aim at minimizing the integral of a running cost  $\psi(x)$  which is a function of the entire vector of mass  $x$ . We will assume that the running cost function  $\psi(x)$  is convex in  $x$ , nondecreasing in each entry  $x_i$ , and such that  $\psi(0) = 0$ . A particularly relevant special case is when the cost function is separable, i.e., when

$$\psi(x) = \sum_{i \in \mathcal{E}} \psi_i(x_i), \quad (1)$$

<sup>1</sup>Each cell is meant to model a portion of an actual road of a given length, so that the graph  $\mathcal{G}$  need not in general coincide with the actual road network topology. In fact  $\mathcal{G}$  may represent a refinement of such actual road network topology, with a given road possibly split into multiple adjacent cells. Observe that such refinement maintains the original intersection layout as well as the original sets of on-ramps and off-ramps.

for convex non-decreasing costs  $\psi_i(x_i)$  of the mass on the single cells  $i \in \mathcal{E}$ , with  $\psi_i(0) = 0$ . We will use the following optimization variables, all function of time:  $x_i$ ,  $y_i$ , and  $z_i$  stand, respectively, for the mass on, the inflow in, and the outflow from, cell  $i \in \mathcal{E}$ ;  $f_{ij}$  stands for the flow between two contiguous cells  $i, j \in \mathcal{E}$  such that  $\sigma_j = \tau_i$ ; and  $\mu_i$  is the the out-flow from an off-ramp  $i \in \mathcal{R}^o$  that leaves the network. Let  $T > 0$  be the given time horizon.

## 2.1 System Optimum Dynamic Traffic Assignment

We first introduce the basic version of the system optimum dynamic network traffic assignment (SO-DTA) problem that can be formulated as follows

$$\min \int_0^T \psi(x(t)) dt \quad (2)$$

such that,

$$x_i(0) = x_i^0, \quad i \in \mathcal{E}, \quad (3)$$

and for all  $t \in [0, T]$ ,

$$\dot{x}_i = y_i - z_i, \quad i \in \mathcal{E}, \quad (4)$$

$$y_i = \lambda_i + \sum_{j \in \mathcal{E}} f_{ji}, \quad z_i = \mu_i + \sum_{j \in \mathcal{E}} f_{ij}, \quad i \in \mathcal{E}, \quad (5)$$

$$\mu_i \geq 0, \quad f_{ij} \geq 0, \quad i, j \in \mathcal{E}, \quad (6)$$

$$f_{ij} = 0 \quad (i, j) \in \mathcal{E} \times \mathcal{E} \setminus \mathcal{A}, \quad (7)$$

$$\mu_i = 0 \quad i \in \mathcal{E} \setminus \mathcal{R}^o,$$

$$y_i \leq s_i(x_i), \quad z_i \leq d_i(x_i), \quad i \in \mathcal{E}. \quad (8)$$

Equation (3) prescribes an initial value of the cell mass  $x_i$ . Equation (4) captures the dynamical constraints that are derived from the law of mass conservation: the time-derivative of the  $x_i$  on a cell equals the imbalance between its inflow  $y_i$  and its outflow  $z_i$ . Equation (5) models flow conservation: it states that the inflow  $y_i$  in a cell is the aggregate of the external inflow  $\lambda_i$  and the flows  $f_{ji}$  from other cells in the network and, symmetrically, the outflow  $z_i$  from a cell is the aggregate of the flows  $f_{ij}$  to other cells in the network and the outflow  $\mu_i$  towards the external world.<sup>2</sup> The inequalities in (6) enforce non-negativity of the cell-to-cell flows  $f_{ij}$  and of the external outflows  $\mu_i$ . Observe that, together with (5) and non-negativity of the external inflows  $\lambda_i$ , equation (6) implies non-negativity of the cells' inflows  $y_i$  and outflows  $z_i$  as well. Equation (7) captures

<sup>2</sup>In fact, one could have replaced  $y_i$  and  $z_i$  in both the right-hand sides of (4) and (8) by the expressions in the right-hand sides in (5) and reduced the number of variables in the SO-DTA problem. However, introducing the variable  $y_i$  and  $z_i$  turns out to be useful for the variants of the DTA discussed in Section 2.2. Using these additional variables also proves useful in deriving distributed optimization algorithms based, e.g., on the alternating method of multipliers or interior point methods, e.g., see [2].

the network topology constraints: the latter require that flows  $f_{ij}$  within the network are possible only between contiguous cells ( $\tau_i = \sigma_j \neq w$ ), and outflows  $\mu_i$  towards the external world are possible only from the off-ramps.<sup>3</sup> Finally, the inequalities in (8) capture the physical constraints on the cells: they guarantee that the total inflow  $y_i$  in a cell does not exceed the supply  $s_i(x_i)$ , and the total outflow  $z_i$  from a cell does not exceed the demand  $d_i(x_i)$ . Because of the assumption  $d_i(0) = 0$  and non-negativity of the cell inflow  $y_i$ , equation (4) implies that the mass  $x_i$  remains nonnegative in time, on every cell  $i \in \mathcal{E}$ .

This form of the SO-DTA problem is a continuous-time version of what was considered by [26] in discrete time and in the special case when the cost

$$\psi(x) = \sum_{i \in \mathcal{E}} x_i \quad (9)$$

is the total traffic volume in the network and the demand functions  $d_i(x_i)$  and supply functions  $s_i(x_i)$  are piecewise affine. In this case —and more in general, for linear, not necessarily identical, cost functions— the optimization problem (2)–(8) is a linear program. In our more general formulation, where the cost  $\psi(x)$  is allowed to be a convex function of the mass vector  $x$  and the demand and supply functions are concave, the optimization problem (2)–(8) is a convex (infinite-dimensional) program. That is, if  $(x^{(0)}, y^{(0)}, z^{(0)}, f^{(0)}, \mu^{(0)})$  and  $(x^{(1)}, y^{(1)}, z^{(1)}, f^{(1)}, \mu^{(1)})$  both satisfy the constraints (3)–(8), then for every  $0 \leq \beta \leq 1$  also  $(x^{(\beta)}, y^{(\beta)}, z^{(\beta)}, f^{(\beta)}, \mu^{(\beta)})$ , where  $x^{(\beta)} = (1 - \beta)x^{(0)} + \beta x^{(1)}$ ,  $y^{(\beta)} = (1 - \beta)y^{(0)} + \beta y^{(1)}$  and so on, satisfies (3)–(8), and has a cost

$$\int_0^T \psi(x^{(\beta)}(t)) dt \leq (1 - \beta) \int_0^T \psi(x^{(0)}(t)) dt + \beta \int_0^T \psi(x^{(1)}(t)) dt.$$

The special case (1) where the cost is separable and convex is suitable for efficient solutions, e.g., based on distributed iterative algorithms [2].

It should be emphasized that the constraints in (3)–(8) neither completely account for realistic traffic dynamics, e.g., as specified by the CTM in [9], nor for variables corresponding to variable speed, ramp metering or routing control. In Section 3, we shall determine values of these controllers so that the optimal solution to SO-DTA is feasible with respect to several well-known models for realistic traffic dynamics, including the CTM, under the designed controllers. Moreover, the SO-DTA problem presumes that the routing of the vehicles on the network is a variable that can be freely optimized by the traffic planner within the only constraints imposed by the exogenous inflows, the network topology, and the cells' physical limits. In the next subsection we restrict the optimization space in the SO-DTA problem to account for additional constraints in the

---

<sup>3</sup>Notice that, because of the assumption that  $\lambda_i \neq 0$  only on on-ramps, and of the first line of (7), it turns out that at most one between the two inflow terms  $\lambda_i$  and  $\sum_j f_{ji}$  appearing in the righthand side of the first equation in (5) can be positive: the external inflow  $\lambda_i$  for onramps  $i \in \mathcal{R}$ , and the aggregate inflow from other cells  $\sum_j f_{ji}$  for every  $i \in \mathcal{E} \setminus \mathcal{R}$ . Similarly, (7) implies that only one of the outflow terms  $\mu_i$  and  $\sum_j f_{ij}$  appearing in the righthand side of the second equation in (5) can be positive: the external outflow  $\mu_i$  for off ramps  $i \in \mathcal{R}^o$ , and the aggregate outflow towards other cells  $\sum_j f_{ij}$  for all  $i \in \mathcal{E} \setminus \mathcal{R}^o$ .

routing due to drivers' choices modeled as exogenous variables, while continuing to postpone the consideration of realistic traffic dynamics and controllers of all these SO-DTA variations to Section 3.

## 2.2 DTA problems with Exogenous Routing Constraints

Let us consider an exogenous, possibly time-varying, routing matrix  $R$ , which is a nonnegative  $\mathcal{E} \times \mathcal{E}$  matrix satisfying the network topology constraints

$$R_{ij} = 0, \quad (i, j) \in (\mathcal{E} \times \mathcal{E}) \setminus \mathcal{A}, \quad (10)$$

and such that

$$\sum_{j \in \mathcal{E}} R_{ij} = 1, \quad i \in \mathcal{E} \setminus \mathcal{R}^o. \quad (11)$$

The matrix  $R$  is to be interpreted as describing the drivers' route choices, with its entries  $R_{ij}$ , sometimes referred to as turning ratios, representing the fractions of flow leaving cell  $i$  that wants to go to cell  $j$ . Equation (11) then guarantees that all the outflow from the non off-ramp cells is split among other cells in the network, while equation (10) guarantees that the outflow from cell  $i$  is split among adjacent downstream cells only.

We will consider two routing-constrained DTA problems. The first one, to be referred as the partially constrained (PC) SO-DTA consists in solving the minimization (2) under the constraints (3)–(8) and the additional constraint

$$f_{ij} \leq R_{ij}d_i(x_i) \quad i, j \in \mathcal{E}. \quad (12)$$

The inequality above requires the flow  $f_{ij}$  from a cell  $i$  to a cell  $j$  not to exceed a given fraction  $R_{ij}$  of the demand  $d_i(x_i)$  on cell  $i$ . Intuitively, if we interpret  $d_{ij}(x_i) = R_{ij}d_i(x_i)$  as the aggregate demand of vehicles on cell  $i$  that want to move from cell  $i$  towards cell  $j$ , then inequality (12) constrains the actual flow  $f_{ij}$  from  $i$  to  $j$  not to exceed such demand. Observe that (12) is a convex constraint so that the (PC) SO-DTA remains a convex program. Clearly, the feasible set of the PC-SO-DTA problem is contained in the one of the SO-DTA problem, which in turn implies that the cost of an optimal solution of the PC-SO-DTA problem is never smaller than the one of an optimal solution of the SO-DTA.

The second routing-constrained DTA problem we propose, to be referred as the fully constrained (FC) SO-DTA consists in solving the minimization (2) under the constraints (3)–(8) and the additional constraint

$$f_{ij} = R_{ij}z_i, \quad i \in \mathcal{E}. \quad (13)$$

The interpretation of (13) is that it forces the outflow from cell  $i$  to split exactly as prescribed by the routing matrix  $R$ , not only when it coincides with the demand  $d_i(x_i)$  (as prescribed by (12)), but also when it is strictly smaller than that —e.g., when the supply constraint of one of the downstream links  $k$  (with  $\sigma_k = \tau_i \neq w$ ) is satisfied with equality. Note that (13) and (8) jointly imply (12). Hence, the feasible set of the FC-SO-DTA problem —which is also convex



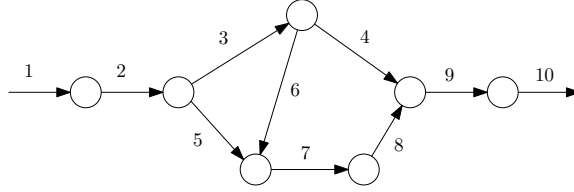


Figure 3: The network used in the numerical study.

since (13) is a linear constraint— is a subset of the feasible set of PC-SO-DTA and, *a fortiori*, of that of the SO-DTA problem. As an immediate consequence, we have the following inequalities

$$\Psi^* \leq \Psi_{PC}^* \leq \Psi_{FC}^*, \quad (14)$$

where  $\Psi^*$ ,  $\Psi_{PC}^*$ , and  $\Psi_{FC}^*$  stand for the costs of an optimal solution of the SO-DTA, the PC-SO-DTA, and FC-SO-DTA, respectively.

### 2.3 Simulations Comparing Various SO-DTA Formulations

In this section, we compare the optimal solutions obtained from the proposed three variants of SO-DTA with the CTM model under FIFO policy as proposed in [9] with proportional merge rule as in [22, 6]. We first provide the details of the simulation setting that are common across this section, and the simulations in Sections 4.1 and 4.2. We solve all the SO-DTA variants in MatLab using the Convex Programming package *cvx* [7, 13]. We use the single-origin single-destination network described in [26] and shown in Figure 3 for our simulations. For implementation, we discretize the continuous formulation according to standard practices in Cell Transmission Models. Time is slotted with sampling time  $\tau = 10$  seconds. In all the cells, demand and supply functions are piecewise affine:

$$d_i(x_i, t) = \min\left\{\frac{v_i x_i}{L_i}, C_i(t)\right\}$$

$$s_i(x_i, t) = \min\left\{\frac{w_i(x_i^{jam} - x_i)}{L_i}, C_i(t)\right\}$$

where  $v_i$ ,  $w_i$ ,  $C_i(t)$ ,  $L_i$  and  $x_i^{jam}$  are the free-flow speed, the wave speed, the capacity (at time  $t = 1, \dots, n$ ), the length and the jam mass on cell  $i$ , respectively. The values of these parameters, along with number of lanes and length of cells, are specified in Table 1. The units of all parameters, as well as of inflows, provided below, are chosen in such a way that physical consistency is ensured. In addition, with the chosen parameters, a vehicle travels along an entire cell in exactly one time slot at maximum speed, which in the considered scenario is the free-flow speed  $v$ . Therefore, the Courant-Friedrichs-Lévy condition  $\frac{\tau \max_i v_i}{\min_i L_i} \leq 1$ , which is necessary for numerical stability, is satisfied.

Parameter	Value
Free-flow speed $v_i$ , wave speed $w_i$	50 feet / sec
Length of cell $L_i$	500 feet
Capacity $C_i$	$6\ell_i$ veh/ $\tau$ (except 4)
Number of lanes $\ell_i$	2 for $i = 1, 2, 9, 10$ ; 1 otherwise
	$10\ell_i$ veh

Table 1: Cell parameters.

Vehicles enter the network from cell 1 at rate  $\lambda_1(t)$ . The setup in this section and Section 4.2 differs from the setup in Section 4.1 in terms of the time-varying values of  $\lambda_1(t)$  and capacities on the links. In this section and Section 4.2, we consider a setting in which<sup>4</sup>  $\lambda_1(1) = 8$ ,  $\lambda_1(2) = 16$ ,  $\lambda_1(3) = 8$  and  $\lambda_1(t) = 0$  for  $t \geq 4$ , with a time horizon of  $T = 25$  steps, and in which the capacity in the cells is constant except on cell 4, where a bottleneck is simulated by setting  $C_4(t) = 6$  veh/ $\tau$  for  $t \neq 5, 6, 7, 8$ ,  $C_4(5) = C_4(6) = 0$  veh/ $\tau$ ,  $C_4(7) = C_4(8) = 3$  veh/ $\tau$ . Exogenous turning ratios are as follows:  $R_{23} = 2/3$ ,  $R_{25} = 1/13$  and  $R_{34} = 2/3$ ,  $R_{36} = 1/3$ , the others being trivial.

For these values of inflow and link capacities, we computed optimal costs for all the three SO-DTA variants and the costs associated with a system evolving under FIFO policy with proportional merge rule. For brevity, we refer to the last model as FIFO. The initial condition for each case was  $x(0) = 0$ . The results for the total traffic volume cost  $\Psi^{(1)}(x) = \sum_t \sum_{i \in \mathcal{E}} x_i(t)$  are reported in Table 2, whereas the results for the quadratic cost,  $\Psi^{(2)}(x) = \sum_t \sum_{i \in \mathcal{E}} x_i^2(t)$ , are reported in Table 3. The corresponding trajectories for volume of vehicles,  $x_i(t)$ , for a few representative cells are shown in Figures 4 and Figures 5 for linear and quadratic cost, respectively.

As expected, the SO-DTA, being the least constrained, gives the least cost, the FC-SO-DTA scheme gives the highest, and the PC-SO-DTA in between, for both linear and quadratic cost criteria. Moreover, again as expected, the optimal cost under any of the SO-DTA variant is no more than the cost under FIFO. This favorable comparison between the optimal costs for the SO-DTA variants and the FIFO model serves as a motivation to investigate the feasibility of optimal SO-DTA solutions with respect to FIFO and other realistic traffic dynamics. We address this issue rigorously in Section 3.

Interestingly, for the linear cost criterion, the FC-SO-DTA optimal cost coincides exactly with the FIFO case. In Proposition 2 in the next section, we show that this is no mere coincidence, and that one can identify a class of settings for which this property can be proven to be true. Finally, we refer to the cost comparison for the quadratic cost criterion in Table 3 to emphasize that this property does not hold true in general.

<sup>4</sup>Inflows are normalized by the onramp length as the dynamics involve the mass of vehicles.

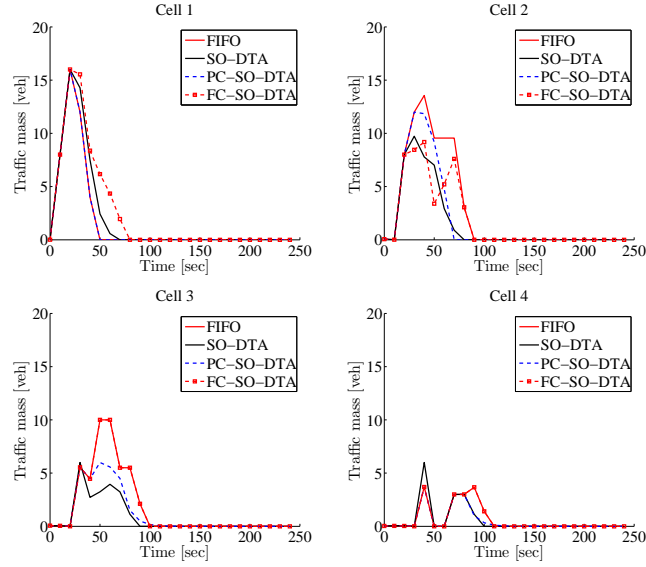


Figure 4: Trajectories of the number of vehicles on cells 1, 2, 3, 4 for the system under FIFO rule and for the optimal solutions corresponding to the three variants of SO-DTA, for linear cost.

Scheme	Cost
FIFO	281.6
SO-DTA	246
PC-SO-DTA	257.1
FC-SO-DTA	281.6

Table 2: Comparison between optimal cost for the three SO-DTA variants, and the cost for the system under FIFO rule, for the linear cost criterion.

Scheme	Cost
FIFO	1930.5
SO-DTA	1393.5
PC-SO-DTA	1537.5
FC-SO-DTA	1595.7

Table 3: Comparison between optimal cost for the three SO-DTA variants, and the cost for the system under FIFO rule, for the quadratic cost criterion.

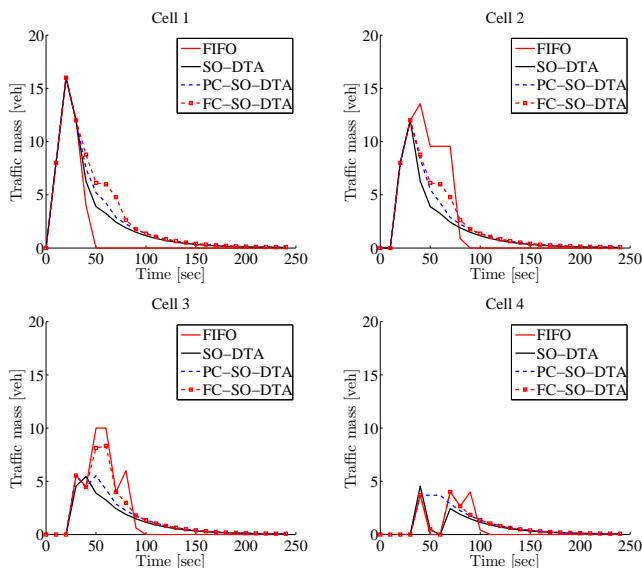


Figure 5: Trajectories of the number of vehicles on cells 1, 2, 3, 4 for the system under FIFO rule and for the optimal solutions corresponding to the three SO-DTA variants, for quadratic cost.

### 3 Control Design and Feasibility of DTA Solutions under Realistic Traffic Dynamics

In this section, we first show how feasible solutions of the SO-DTA, of the PC-SO-DTA, and of the FC-SO-DTA problems are feasible with respect to realistic cell-based Dynamic Network Loading (DNL) models using proper control inputs. The control inputs we consider for the FC-SO-DTA consist in a combination of ramp metering on the on-ramps and variable speed limits on the other cells. On the other hand, for the SO-DTA and the PC-SO-DTA, we also consider routing controls. We then focus on the FC-SO-DTA problem in the special case when the network consists of only simple, merge, and diverge intersections, and whose cells have linear demand functions and affine supply functions with identical slope. We show that, in this special case, the optimal solution to the constrained SO-DTA with total traffic volume as cost, is readily feasible with respect to the FIFO DNL model.

#### 3.1 Feasibility of DTA Solution under Realistic Traffic Dynamics

We start by discussing the considered control strategies. We will assume that the controller has the ability to reduce the demand functions setting controlled

demand functions in the form

$$\bar{d}_i(x_i) = \alpha_i d_i(x_i), \quad i \in \mathcal{E} \setminus \mathcal{R} \quad (15)$$

$$\bar{d}_i(x_i) = \min\{d_i(x_i), c_i\}, \quad i \in \mathcal{R} \quad (16)$$

where  $\alpha_i \in [0, 1]$  and  $c_i \geq 0$  are control parameters. In the context of freeway networks, (15)–(16) can be realized through appropriate setting of speed limits and ramp metering. In particular, for linear uncontrolled demand functions  $d_i(x_i) = v_i x_i$ , formula (15) is equivalent to the modulation of the free-flow speed  $\bar{v}_i = v_i \alpha_i$ , where  $v_i$  could be interpreted as the maximum possible speed due to, e.g., safety considerations (Cf., e.g., [14]). On the other hand, (16) corresponds to metering the maximum outflow from the onramp, which is its demand  $d_i(x_i)$ , by imposing a maximum value  $c_i$  (Cf., e.g., [22]).

While control of the demand functions as above proves to be sufficient to ensure feasibility of the solutions of the FC-SO-DTA with a given exogenous turning ratio matrix  $R$  (cf. Proposition 1 point (iii)), implementation of the solutions of the SO-DTA and of the PC-SO-DTA require additional actuation capabilities that allow for the design of a controlled turning ratio matrix  $\bar{R}$  whose entries are nonnegative and satisfy the constraints (10) and (11). For consistency in notation, we will let  $\bar{R} = R$  when discussing implementations of the FC-SO-DTA.

We now discuss the considered DNL models. For transportation systems, the term DNL generally refers to the modeling of the circular dependance between the network flow propagation and the link performance (cf., e.g., [3, Chapter 7]). In the specific framework considered in this paper, such circular dependance is modeled by the differential equation (4), coupled with a functional dependence

$$f_{ij} = f_{ij}(x, \alpha, c, \bar{R}), \quad (i, j) \in \mathcal{A}, \quad \mu_k = \mu_k(x, \alpha), \quad k \in \mathcal{R}^o$$

of the cell-to-cell flows and of the external outflows as a function of the cell mass and the control parameters. In particular, we will focus on DNL models such that the external outflow from the off-ramps always coincides with their (controlled) demand, i.e.,

$$z_k = \mu_k = \bar{d}_k(x_k), \quad k \in \mathcal{R}^o; \quad (17)$$

and the outflow from every cell coincides with the controlled demand in the *free-flow region*, i.e.,

$$x \in \mathcal{F} \quad \implies \quad z_i = \bar{d}_i(x_i), \quad \forall i \in \mathcal{E}, \quad (18)$$

where  $\mathcal{F}$  denotes the free-flow region

$$\mathcal{F} := \left\{ x \in \mathbb{R}_+^{\mathcal{E}} : \sum_{i \in \mathcal{E}} \bar{R}_{ij} \bar{d}_i(x_i) \leq s_j(x_j), \forall j \in \mathcal{E} \right\}. \quad (19)$$

The considered DNL models differ for the way the cell-to-cell flows depend on the cell mass and on the control parameters in the congestion regime, i.e., when  $\sum_{i \in \mathcal{E}} \bar{R}_{ij} \bar{d}_i(x_i) > s_j(x_j)$  for some cell  $j \in \mathcal{E}$ . Among the several possibilities, we will consider two specific cases:

1. the FIFO model

$$f_{ij}^F = \bar{R}_{ij} z_i^F, \quad z_i^F = \gamma_i^F \bar{d}_i(x_i), \quad (i, j) \in \mathcal{A}, \quad (20)$$

where for all  $i \in \mathcal{E}$

$$\gamma_i^F = \sup \left\{ \gamma \in [0, 1] : \gamma \cdot \max_{\substack{k \in \mathcal{E}: \\ (i, k) \in \mathcal{A}}} \sum_{h \in \mathcal{E}} \bar{R}_{hk} \bar{d}_h(x_h) \leq s_k(x_k) \right\} \quad (21)$$

2. and the non-FIFO model

$$f_{ij}^N = \gamma_j^N \bar{R}_{ij} \bar{d}_i(x_i), \quad (i, j) \in \mathcal{A}, \quad (22)$$

where for all  $j \in \mathcal{E}$

$$\gamma_j^N = \sup \left\{ \gamma \in [0, 1] : \gamma \cdot \sum_{h \in \mathcal{E}} \bar{R}_{hj} \bar{d}_h(x_h) \leq s_j(x_j) \right\} \quad (23)$$

The FIFO DNL model (20)-(21) generalizes Daganzo's cell-transmission model [9] by extending it to the case where nodes (i.e., junctions) may have multiple incoming and outgoing links (cells)<sup>5</sup> and the cells' demand and supply functions are allowed to be concave.<sup>6</sup> Since  $f_{ij}^F = \bar{R}_{ij} z_i^F$  in every circumstances, the FIFO DNL is amenable to the modeling of multi-origin multi-destination transportation networks. However, as pointed out by some authors [10], it corresponds to a rather conservative behavioral model, in which not only drivers never change their routing choice, thus blindly queuing up even in presence of alternative routes to the same destination, but more importantly it does not take into account presence of multiple lanes for multiple manoeuvres at junctions. For example, a congested offramp on a freeway would slow down and possibly block the flow of vehicles on the main line, which is not always realistic.

On the other hand, the main difference of the non-FIFO model with respect to the FIFO one is that congestion in one of the outgoing cells does not influence the flow towards other outgoing cells. In the previous example, while the congested offramp forces vehicles that would like to take it to stop in the freeway, those that want to continue on the main line are free to do so, if the downstream supply of the main line is sufficient. In fact, the non-FIFO DNL model satisfies  $f_{ij}^N = \bar{R}_{ij} z_i^N$  when  $z_i^N = \bar{d}_i(x_i)$  (free-flow regime), whereas the actual turning ratios  $f_{ij}^N / z_i^N$  may deviate from the prescribed ones, namely,

<sup>5</sup>Daganzo [9] considers only the cases of nodes with single incoming link (diverge junction) or single outgoing link (merge junction). It is easily seen that, for diverge junctions (20)-(21) prescribe that the outflow from a diverge junction always splits into the downstream cells according to the turning ratios, and the supply of a congested merge junction is allocated according to a proportional rule. This is a slight variation with respect to the original CTM model [9], in which merge is solved via a priority rule.

<sup>6</sup>In Daganzo's original cell-transmission model [8], demand functions are linear and supply functions are affine.

$\bar{R}_{ij}$ , when  $z_i^N < \bar{d}_i(x_i)$  (congested regime). As a consequence, the non-FIFO DNL model can be used for single-origin single-destination network (in which the actual path of a vehicle does not matter), but exhibits unrealistic behaviors in multi-origin multi-destination networks. A possibly more realistic model may involve a combination of the two DNL models —FIFO and non-FIFO— in which a fraction of drivers can change path, while another fraction cannot – for example, private cars can deviate from their path to chose a more convenient one, while buses or trucks have prescribed paths to follow.

To summarize, we consider DNL models that can all be written in the following form

$$\dot{x}_i(t) = \lambda_i(t) + g_i^M(x(t), \alpha(t), c(t), \bar{R}(t)), \quad i \in \mathcal{E}, \quad (24)$$

for all  $t \in [0, T]$ , where  $\lambda_i(t)$  is the external inflow in cell  $i$ ,  $\alpha(t)$  is the vector of all demand control parameters,  $c(t)$  is the vector of all ramp metering control parameters, and  $\bar{R}(t)$  is the controlled turning ratio matrix; the superscript  $M$  indexes the specific model (i.e.,  $M = F$  for FIFO,  $M = N$  for non-FIFO);

$$g_i^M(x, \alpha, c, \bar{R}) = \sum_{j \in \mathcal{E}} f_{ji}^M(x, \alpha, c, \bar{R}) - z_i^M, \quad z_i^M = \begin{cases} \sum_{j \in \mathcal{E}} f_{ij}^M(x, \alpha, c, \bar{R}) & i \in \mathcal{E} \setminus \mathcal{R}^o \\ \mu_i & i \in \mathcal{R}^o \end{cases} \quad (25)$$

and the outflows  $z_i^M$  satisfy (18).

We now address the issue of implementation of the optimal solutions to the SO-DTA, the PC-SO-DTA, and the FC-SO-DTA problems of Section 2. Our result is summarized in the following Proposition.

**Proposition 1**

- (i) For any feasible solution  $(x_i(t), y_i(t), z_i(t), \mu_i(t), f_{ij}(t))$  of the SO-DTA problem (3)-(8), set the demand controls  $\alpha_i(t)$ , ramp metering controls  $c_i(t)$ , and controlled turning ratio matrix  $\bar{R}(t)$ , for  $t \in [0, T]$ , as follows

$$\alpha_i(t) = \frac{z_i(t)}{d_i(x_i(t))}, \quad \forall i \in \mathcal{E} \setminus \mathcal{R} \quad (26)$$

$$c_i(t) = z_i(t), \quad \forall i \in \mathcal{R} \quad (27)$$

$$\bar{R}_{ij}(t) = \frac{f_{ij}(t)}{z_i(t)}, \quad \forall i, j \in \mathcal{E} \quad (28)$$

with the convention that  $\alpha_i(t) = 1$  if  $z_i(t) = d_i(x_i(t)) = 0$  and that, if  $z_i(t) = 0$ , then  $\bar{R}_{ij}(t) = |\{k \in \mathcal{E} : (i, k) \in \mathcal{A}\}|^{-1}$  for all  $(i, j) \in \mathcal{A}$  and  $R_{ij}(t) = 0$  for all  $(i, j) \notin \mathcal{A}$ . Then  $x(t)$  coincides with the trajectory of the controlled DNL model (24)–(25).

Moreover, let  $R(t)$ ,  $t \in [0, T]$ , be an exogenous turning ratio matrix. Then:

(ii) For any feasible solution  $(x_i(t), y_i(t), z_i(t), \mu_i(t), f_{ij}(t))$  of the PC-SO-DTA problem (3)-(8) and (12), set the demand controls  $\alpha_i(t)$  and controlled turning ratio matrix  $\bar{R}(t)$ , for  $t \in [0, T]$ , as in (26) and (28), respectively. Then, the following is satisfied:

$$\alpha_i \bar{R}_{ij} \leq R_{ij}, \quad i, j \in \mathcal{E}, i \notin \mathcal{R}. \quad (29)$$

and  $x(t)$  coincides with the trajectory of the controlled DNL model (24)–(25).

(iii) For any feasible solution  $(x_i(t), y_i(t), z_i(t), \mu_i(t), f_{ij}(t))$  of the FC-SO-DTA problem (3)-(8) and (13), set the demand controls  $\alpha_i(t)$ , for  $t \in [0, T]$ , as in (26), and let controlled turning ratio matrix  $\bar{R}(t) = R(t)$  coincide with the uncontrolled one. Then,  $x(t)$  coincides with the trajectory of the controlled DNL model (24)–(25).

Furthermore, in all the three cases (i)–(iii) above, the implemented trajectory is in the free-flow region at all times, i.e.,  $x(t) \in \mathcal{F}$  for all  $t \in [0, T]$ .

Proposition 1 provides a methodology to take any feasible solution of any of the three convex SO-DTA variants considered in Section 2, and make it feasible with respect to general DNL models, for concave demand and supply functions, and for general network structures. As such, this generalizes existing results, e.g., see [22], which are applicable only in specific scenarios. The proof of Proposition 1 is provided in Appendix A.1. In particular, for the PC-SO-DTA problem, equation (29) can be used to quantify the coupling between the deviation of the designed routing matrix  $\bar{R}$  from the prescribed routing matrix  $R$  and variable speed limit control. E.g., when the speed limit is not reduced, i.e.,  $\alpha_i = 1$ , the entries of  $\bar{R}$  corresponding to routing from link  $i$  to its downstream cells coincide with the corresponding entries of  $R$ , and the possibility for deviation increases with decreasing speed limit.

### 3.2 Analysis of the FC-SO-DTA problem

In this subsection, we apply optimal control techniques to the study of the FC-SO-DTA problem (2)–(8) and (13). As a first step, it proves convenient to use the outflows  $z_i$  as the only optimization variables and substitute  $f_{ij} = R_{ij}z_i$  for  $i, j \in \mathcal{E}$ ,  $\mu_k = z_k$  for  $k \in \mathcal{R}^o$ , and  $y_i = \lambda_i + \sum_j R_{ji}z_j$  for  $i \in \mathcal{E}$ . Then, the FC-SO-DTA problem can be formulated as

$$\begin{aligned} & \min \int_0^T \psi(x(t)) dt \\ & x_i(0) = x_i^0, \quad i \in \mathcal{E}, \\ & \dot{x}_i = \lambda_i + \sum_{j \in \mathcal{E}} R_{ji}z_j - z_i, \quad i \in \mathcal{E}, \\ & z_i \geq 0, \quad \sum_{j \in \mathcal{E}} R_{ji}z_j \leq s_i(x_i), \quad z_i \leq d_i(x_i), \quad i \in \mathcal{E}. \end{aligned} \quad (30)$$



The Hamiltonian associated to FC-SO-DTA problem (30) is given by

$$H(x, z, \zeta) = \psi(x) + \sum_{i \in \mathcal{E}} \zeta_i \left( \lambda_i + \sum_{j \in \mathcal{E}} R_{ji} z_j - z_i \right), \quad (31)$$

where  $x$  is the state vector,  $z$  is the control vector, and  $\zeta$  is the adjoint state vector. Upon introducing the notation

$$\kappa_i = \zeta_i - \sum_{j \in \mathcal{E}} R_{ij} \zeta_j, \quad i \in \mathcal{E},$$

the Hamiltonian can be rewritten as

$$H(x, z, \zeta) = \psi(x) + \sum_{i \in \mathcal{E}} \zeta_i \lambda_i - \sum_{i \in \mathcal{E}} \kappa_i z_i. \quad (32)$$

Then, the Pontryagin maximum principle implies the following necessary condition: if  $(x^*, z^*)$  is an optimal solution of (30), then, for every  $t \in [0, T]$ ,

$$\begin{aligned} z^* \in \underset{(z_i)_{i \in \mathcal{E}}}{\operatorname{argmin}} \quad & H(x^*, z, \zeta) = \underset{(z_i)_{i \in \mathcal{E}}}{\operatorname{argmax}} \quad \sum_{i \in \mathcal{E}} \kappa_i z_i. \quad (33) \\ 0 \leq z_i \leq d_i(x_i^*) \quad & 0 \leq z_i \leq d_i(x_i^*) \\ \sum_{j \in \mathcal{E}} R_{ji} z_j \leq s_i(x_i^*) \quad & \sum_{j \in \mathcal{E}} R_{ji} z_j \leq s_i(x_i^*) \end{aligned}$$

For a given value of the state  $x$  and of the adjoint state  $\zeta$ , the optimization in rightmost side of (33) is a linear problem in the variables  $z_i$ . If one denotes by  $\xi_i$  and  $\nu_i$  the multipliers associated to, respectively, the demand and the supply constraints, then the dual problem to one in the rightmost side of (33) can be written as

$$\begin{aligned} (\xi^*, \nu^*) \in \underset{(\xi_i, \nu_i)_{i \in \mathcal{E}}}{\operatorname{argmin}} \quad & \sum_{i \in \mathcal{E}} (\xi_i d_i(x_i^*) + \nu_i s_i(x_i^*)), \quad (34) \\ \xi_i \geq 0, \nu_i \geq 0 \quad & \\ \xi_i + \sum_{j \in \mathcal{E}} R_{ij} \nu_j \geq \kappa_i \quad & \end{aligned}$$

and the adjoint dynamical equations read

$$\dot{\zeta}_i = -\frac{\partial}{\partial x_i} \psi(x^*) + \xi_i^* d'_i(x_i^*) + \nu_i^* s'_i(x_i^*), \quad i \in \mathcal{E}, \quad (35)$$

where  $d'_i(x_i)$  and  $s'_i(x_i)$  are the derivatives of the demand and, respectively, of the supply functions, with transversality condition

$$\zeta_i(T) = 0, \quad i \in \mathcal{E}. \quad (36)$$

If every node  $v$  in the network is either an ordinary junction (single incoming and outgoing cell), a merge junction (multiple incoming and single outgoing cells),

or a diverge junction (single incoming and multiple outgoing cells), then it is convenient to regroup the addends of the summation appearing in the rightmost side of (33) so that the necessary condition for optimality can be separated into decoupled local linear programs

$$\begin{aligned} (z_i^*)_{i:\tau_i=v} \in & \operatorname{argmax}_{(z_i)_{i:\tau_i=v}} \sum_{i:\tau_i=v} \kappa_i z_i, \quad \forall v \in \mathcal{V}. \quad (37) \\ & 0 \leq z_i \leq d_i(x_i^*) \\ & \sum_{i:\tau_i=v} R_{ij} z_i \leq s_j(x_j^*), \quad \forall j: \sigma_j = v \end{aligned}$$

In the special case where the cost is the total volume, demand is linear and supply functions are affine, all with identical slopes, equations (35)–(37) imply the following result on the structure of the optimal control.

**Proposition 2** *Let the cost function be as in (9), the demand functions be  $d_i(x_i) = \omega x_i$ , and the supply functions have the form  $s_i(x_i) = \theta_i - \omega x_i$  for some  $\theta_i > 0$  and  $\omega > 0$ . Let  $R$  be a routing matrix that is constant in time, and let  $(x^*, z^*)$  be an optimal solution of the corresponding FC-SO-DTA. Then, for every non off-ramp cell  $i \in \mathcal{E} \setminus \mathcal{R}_o$ ,*

(i) *if  $v = \tau_i$  is an ordinary junction with downstream cell  $j$  (with  $\sigma_j = v$ ), then*

$$z_i^* = \min\{d_i(x_i^*), s_j(x_j^*)\}; \quad (38)$$

(ii) *if  $v = \tau_i$  is a diverging junction, then*

$$z_i^* = \gamma_i^F d_i(x_i^*), \quad \gamma_i^F = \sup \{\gamma \in [0, 1] : \gamma R_{ik} d_i(x_i^*) \leq s_k(x_k^*), \forall k \in \mathcal{E}\}; \quad (39)$$

(iii) *if  $v = \tau_i$  is a merging junction with downstream cell  $j$  (with  $\sigma_j = \tau_i$ ), then*

$$\begin{aligned} (z_h^*)_{h:\tau_h=v} \in & \operatorname{argmax}_{(z_h)_{h:\tau_h=v}} \sum_{h \in \mathcal{E}: \tau_h=v} \kappa_h z_h. \quad (40) \\ & 0 \leq z_h \leq d_h(x_h^*) \\ & \sum_{h \in \mathcal{E}: \tau_h=v} z_h \leq s_j(x_j^*) \end{aligned}$$

Proposition 2 implies that at diverging junctions of a transportation network with total traffic volume as cost, affine supply functions and linear demand with identical slope, the optimal solution satisfies

$$f_{ij}^* = R_{ij} \gamma_i^F d_i(x_i^*), \quad \gamma_i^F = \sup \{\gamma \in [0, 1] : \gamma R_{ik} d_i(x_i^*) \leq s_k(x_k^*), \forall k \in \mathcal{E}\},$$

which coincides with the FIFO diverge rule of Daganzo's cell transmission model. Similarly, for merging junctions with two upstream cells  $h$  and  $i$  and downstream cell  $j$ , (40) is equivalent to Daganzo's priority rule

$$f_{ij}^* = \operatorname{mid}\{d_i(x_i^*), s_j(x_j^*) - d_h(x_h^*), p_i s_j(x_j^*)\}$$

and

$$f_{hj}^* = \text{mid}\{d_h(x_h^*), s_j(x_j^*) - d_i(x_i^*), p_h s_j(x_j^*)\},$$

where  $\text{mid}\{a, b, c\}$  denotes the median and the priority parameters  $p_h$  and  $p_i$  are such that:  $p_i = 1$  and  $p_h = 0$  if  $\kappa_i > \kappa_h$ ;  $p_i = 0$  and  $p_h = 1$  if  $\kappa_i < \kappa_h$ ; and  $p_i = 1 - p_h$  is arbitrary in  $[0, 1]$  if  $\kappa_i = \kappa_h$ .<sup>7</sup>

Proposition 2 and the discussion following it imply that, if the demand and supply functions are linear with identical slope, the optimal solution of the FC-SO-DTA problem with total traffic volume as cost is feasible for the CTM with FIFO rule at the diverge junctions, with no additional control required. In particular variable speed limit is not necessary in this specific scenario; however, since the optimal solution under variable speed limit control is guaranteed to be in free-flow (Proposition 1), it can possibly improve safety and reduce environmental footprint

## 4 Robustness analysis

In this section, we first investigate (Section 4.1) the robustness of optimal DTA solutions, which are feasible under control strategies and DNL models described in Section 3.1, with respect to perturbations of the initial condition  $x^0$  and the external inflows  $\lambda_i(t)$ . We then show through numerical simulations how better robustness can be achieved at the expense of some performance loss by shrinking the feasible set of the DTA problems (Section 4.2).

### 4.1 Robustness Analysis of Optimal DTA Solutions

In Section 3, we discussed implementation of optimal solutions to the three versions of DTA problem proposed in Sections 2.1 and 2.2. In order to compute such solutions, one needs precise information about the input parameters, i.e., the initial condition  $x^0$  and external inflow vector  $\lambda(t)$  over the planning horizon  $[0, T]$ . However, in practice, information about these quantities inevitably involves uncertainties. Therefore, a reasonable strategy is to (i) compute the optimal DTA solution for *nominal* values of the external inflows and initial condition, and (ii) compute the corresponding nominal control inputs using Proposition 1; and then expect the trajectory under actual parameter values and the nominal control inputs to be close enough to the nominal trajectory. In this section, we provide formal guarantees on the robustness of a general system trajectory to perturbations in the initial condition and the external inflows, while maintaining the same control input.<sup>8</sup> When specialized to the system trajectory corresponding to the optimal DTA solution under nominal values of the initial condition and external inflows, this gives the desired result on robustness analysis of optimal DTA solution with respect to uncertainties in the input parameters.

<sup>7</sup>In fact, when  $\kappa_i = \kappa_h$ , the proportional rule  $f_{ij} = d_i(x_i^*) \min\{1, s_j(x_j^*)/(d_i(x_i^*) + d_h(x_h^*))\}$ ,  $f_{hj} = d_h(x_h^*) \min\{1, s_j(x_j^*)/(d_i(x_i^*) + d_h(x_h^*))\}$  also satisfies (40).

<sup>8</sup>We recall that the control inputs are open loop, and not in feedback form.

Our analysis is to be contrasted with standard sensitivity analysis for ordinary differential equations. A key difference is that these methods are local, whereas we wish to study relatively large perturbations and over relatively long time horizons. In order to differentiate from the sensitivity analysis literature, we refer to our perturbation bounds as robustness analysis.

We shall use the notational convention that  $x^0$  and  $\lambda(t)$  denote the *nominal* values of the initial condition and the external inflows, while  $\tilde{x}^0$  and  $\tilde{\lambda}(t)$  denote the perturbed values of these parameters. Similarly  $x(t)$  and  $\tilde{x}(t)$  will, respectively, denote the nominal and perturbed trajectories, under the same open-loop control inputs  $\alpha(t)$ ,  $c(t)$  and  $\bar{R}(t)$ . Our robustness analysis will provide bounds on perturbations in the state trajectory due to perturbations in the inflow  $\tilde{\lambda} - \lambda$  and the perturbations in initial condition  $\tilde{x}^0 - x^0$ . The bounds derived in the general setting, when specialized to the case where  $x(t)$  corresponds to an optimal DTA solution and where  $\alpha(t)$ ,  $c(t)$  and  $\bar{R}(t)$  are derived from  $x(t)$  according to Proposition 1, will give the desired robustness analysis for optimal DTA solutions.

Our technique relies on leveraging a certain *monotonicity* property of the dynamical system underlying our DNL model in (24). Monotone systems are dynamical systems whose trajectories preserve the partial order between initial conditions and external inputs. Specifically, for monotone DNL models, trajectories with initial conditions<sup>9</sup>  $x^0 \leq \tilde{x}^0$ , and inflows  $\lambda(t) \leq \tilde{\lambda}(t)$  for all  $t \in [0, T]$ , are such that  $x(t) \leq \tilde{x}(t)$  for all  $t \in [0, T]$ . A standard result in dynamical systems theory, known as Kamke's theorem [16, Theorem 1.2], implies that the DNL model (24) is monotone in a certain domain  $\mathcal{D} \subseteq \mathcal{R}_+^{\mathcal{E}}$  if and only if

$$\frac{\partial g_i^M}{\partial x_j}(x, \alpha, c, \bar{R}) \geq 0, \quad \forall i \neq j \in \mathcal{E}, \quad (41)$$

for almost every  $x \in \mathcal{D}$ .

**Remark 1 (Monotonicity regions of DNL models)** *It is possible to check that, under non-FIFO DNL model, the system is monotone almost everywhere in  $\mathcal{D} = \mathbb{R}_+^{\mathcal{E}}$ , e.g., see [19]. This is because an increase in mass in an outgoing link does not decrease the flow towards other outgoing links at the same intersection.*

*On the other hand, it has been recognized, e.g., see [6], that the FIFO DNL models are monotone in the free-flow region defined in (19), but the property is not satisfied in the region where there exists at least one cell  $k$  outgoing from a diverge junction (i.e., a cell  $k$  such that there are other cells  $j \neq k$  with  $\sigma_j = \sigma_k$ ) that is congested, i.e.,  $\sum_{h \in \mathcal{E}} \bar{R}_{hk} \bar{d}_h(x_h) > s_k(x_k)$ . In fact, in such a configuration, monotonicity is lost since an increase of the mass  $x_k$  in a congested cell  $k$  has the effect of reducing its supply  $s_k(x_k)$ , and thus the coefficient  $\gamma_i^F$  (as defined in (21)) of any upstream cell  $i$  such that  $(i, k) \in \mathcal{A}$ . In turn, this implies a reduction of the flow  $f_{ij}^F$  from any such cell  $i$  to any other downstream cell  $j$  such that  $(i, j) \in \mathcal{A}$ , hence a reduction in the inflow on cell  $j$ .*

<sup>9</sup>Here by  $a \leq b$  for vectors in  $\mathbb{R}^{\mathcal{E}}$  we mean  $a_i \leq b_i$  for all  $i \in \mathcal{E}$ .

Given an  $n$ -dimensional vector  $x$ , recall that its  $\ell_1$  norm is given by  $\|x\|_1 := \sum_{i=1}^n |x_i|$ . For example,  $\|\tilde{x}^0 - x^0\|_1 = \sum_{i \in \mathcal{E}} |\tilde{x}_i^0 - x_i^0|$ , and  $\|\tilde{x}(t) - x(t)\|_1 = \sum_{i \in \mathcal{E}} |\tilde{x}_i(t) - x_i(t)|$  for all  $t \in [0, T]$ . We let  $\|\lambda - \tilde{\lambda}\|_{1,t} := \int_0^t \|\lambda(s) - \tilde{\lambda}(s)\|_1 ds$ .

**Proposition 3** *If*

- (a) *DNL model is non-FIFO; or*
- (b) *DNL model is FIFO, and the perturbations  $\|\tilde{x}^0 - x^0\|_1$  and  $\|\tilde{\lambda} - \lambda\|_{1,T}$  are sufficiently small,*

*then*

$$\|\tilde{x}(t) - x(t)\|_1 \leq \|\tilde{x}^0 - x^0\|_1 + \|\tilde{\lambda} - \lambda\|_{1,t}, \quad \forall t \in [0, T]. \quad (42)$$

For FIFO DNL model, the sufficiently small condition in Proposition 3 is to ensure that the perturbed trajectories remain in free-flow, and hence the system is monotone along them. As already mentioned in Remark 1, non-FIFO DNL models satisfy the monotonicity property everywhere, and hence the smallness condition is not necessary. The bound provided by Proposition 3 has the desirable property that the right hand side of (42) goes to zero as the magnitude of perturbations go to zero. However, the bound is conservative for non-negligible values of perturbations. The next result provides a tighter bound in this latter case. In preparation for it, let  $\|\lambda_i - \tilde{\lambda}_i\|_\infty := \sup_{t \in [0, T]} |\lambda_i(t) - \tilde{\lambda}_i(t)|$ ,  $i \in \mathcal{R}$ , and

$$\bar{\lambda}_i := \sup_{t \in [0, T]} \{\lambda_i(t) + \|\lambda_i - \tilde{\lambda}_i\|_\infty\}, \quad \underline{\lambda}_i := \max\{0, \inf_{t \in [0, T]} \{\lambda_i(t) - \|\lambda_i - \tilde{\lambda}_i\|_\infty\}\}, \quad i \in \mathcal{R}$$

$$\bar{x}_i^0 := x_i^0 + |x_i^0 - \tilde{x}_i^0|, \quad \underline{x}_i^0 := \max\{0, x_i^0 - |x_i^0 - \tilde{x}_i^0|\}, \quad i \in \mathcal{E}$$

Note that the extreme values of perturbed inflows,  $\bar{\lambda}$  and  $\underline{\lambda}$ , are constant. The next bound is expressed in terms of equilibrium masses at these extreme values, denoted as  $x^{eq}(\bar{\lambda})$  and  $x^{eq}(\underline{\lambda})$ . Existence and uniqueness of these equilibria are discussed in [6] for FIFO DNL models and in [19] for non-FIFO DNL models. While in the former, if it exists, the equilibrium is unique, in the latter, manifold of equilibria might appear. Nonetheless, the following result holds for any such equilibria.

**Proposition 4** *If  $\|\tilde{x}^0 - x^0\|_1$  and  $\|\tilde{\lambda} - \lambda\|_{1,T}$  are sufficiently small, and  $x^{eq}(\bar{\lambda})$  and  $x^{eq}(\underline{\lambda})$  exist, then*

$$\|\tilde{x}(t) - x(t)\|_1 \leq \|x^{eq}(\bar{\lambda}) - x^{eq}(\underline{\lambda})\|_1 + \|\tilde{x}^0 - \underline{x}^0\|_1 + \min_{\xi \in \tilde{x}^0, \underline{x}^0} \{\|x^{eq}(\underline{\lambda}) - \xi\|_1 + \|x^{eq}(\bar{\lambda}) - \xi\|_1\} \quad \forall t \in [0, T]. \quad (43)$$

Again, in Proposition 4, the smallness of the perturbations is required to ensure that the perturbed trajectories remain in the free-flow region for FIFO DNL models, and that the corresponding extreme values of inflows admit equilibria.

**Remark 2** *The optimal solution  $x(t)$  to any of the three SO-DTA variants considered in the paper is in free flow for traffic flow dynamics under the control policies  $(\alpha, c, \bar{R})$  designed in Proposition 1. Hence, Propositions 3 and 4 are applicable when the nominal trajectory  $x(t)$  corresponds to the evolution of the system trajectory under the control policies designed in Proposition 1.*

Note that the right hand side of (43) does not go to zero as perturbations go to zero. However, for non-negligible perturbations, it gives less conservative upper bound than (42). Therefore, we propose to use the bound equal to the minimum of the right hand sides of (42) and (43). Indeed, this is the upper bound we use for comparison with simulation results at the end of this subsection.

The perturbations for which Propositions 3 and 4 are not applicable typically result in an *overload* condition, where the perturbed external inflow exceeds network capacity. In such a scenario, the mass on the on-ramps grow unbounded. In our previous work [5, Proposition 2], we characterized this growth rate for a related dynamical network flow model. Inspired by our previous work, we suggest a simple upper bound in the overload regime, for networks with a single on-ramp, e.g., as shown in Figure 3, and with constant values for nominal and perturbed external inflow. The suggested upper bound will be compared in the final part of this subsection against simulation results. Let  $\hat{\lambda}$  be the supremum of all perturbed external inflows under which the perturbed trajectories remain in free-flow, and hence for which Propositions 3 and 4 are applicable. Let  $\hat{x}$  denote the perturbed trajectory under perturbed inflow  $\hat{\lambda}$ . Triangle inequality implies that

$$\|\tilde{x}(t) - x(t)\|_1 \leq \|\hat{x}(t) - x(t)\|_1 + \|\tilde{x}(t) - \hat{x}(t)\|_1 \quad \forall t \geq 0. \quad (44)$$

The first term in (44) can be upper bounded using Propositions 3 and 4. In the second term, the total mass on on-ramps grows unbounded at a rate which is expected to be equal to  $\|\tilde{\lambda} - \hat{\lambda}\|_1 = \sum_{i \in \mathcal{R}^o} |\tilde{\lambda}_i - \hat{\lambda}_i|$ , i.e.,

$$\limsup_{t \rightarrow \infty} \frac{\|\tilde{x}(t) - \hat{x}(t)\|_1}{t} = \|\tilde{\lambda} - \hat{\lambda}\|_1. \quad (45)$$

Since (45) gives a reasonable upper bound for large  $t$ , considering the relatively large time horizon for the simulations, we shall use

$$\|\tilde{x}(t) - \hat{x}(t)\|_1 \leq \|\tilde{\lambda} - \hat{\lambda}\|_1 t \quad (46)$$

for all  $t$ . In summary, the upper bound for the overload regime used in the simulations below is obtained from (44) and (46).

We now compare the robustness bounds obtained in Propositions 3 and 4, and in (44) and (46), with simulation results. We performed simulations for a constant inflow scenario where the nominal value of the inflow is  $\lambda_1(t) = 5$  for all  $t = 0, 1, \dots, T$ ,  $T = 200$ , and in which the link capacities are as in Section 2.3, except that  $C_4(t) = 6 \text{ veh}/\tau$  for all  $t$ , i.e., we do not consider any bottleneck in this section.

For these parameters, and for the total traffic volume cost  $\psi(x) = \sum_{i \in \mathcal{E}} x_i$ , we solve the PC-SO-DTA with initial condition  $x(0) = 0$ , and compute the corresponding controls, as given by Proposition 1. We then compute the cost for the FIFO and non-FIFO DNL models under these controls, but under perturbed inflow  $\tilde{\lambda}_1(t) = \lambda_1(t) + \Delta\lambda$ . We emphasize that the controls do not change with  $\Delta\lambda$ . Let the optimal trajectory, i.e., the solution of PC-SO-DTA, be denoted as  $x^*(t)$ , and the trajectory under perturbed inflow  $\Delta\lambda$  be denoted as  $\tilde{x}^{(\Delta\lambda)}(t)$ . (Note that  $x^0(t) = x^*(t)$ ). We compute the resulting perturbation in cost  $\Delta\Psi(\Delta\lambda) = \sum_{t=0}^{200} \sum_{i \in \mathcal{E}} (\tilde{x}_i^{(\Delta\lambda)}(t) - x_i^*(t))$  for various values of  $\Delta\lambda$  in  $[0, 3]$ .

The results are shown in Figure 6. The solid line plots for the FIFO as well as the non-FIFO models in Figure 6 are piece-wise affine, with the transition point corresponding to network capacity. This transition point is at  $\Delta\lambda \approx 0.8$  and  $\Delta\lambda \approx 2.8$  for the FIFO and non-FIFO DNL models, respectively. In fact, when  $\Delta\lambda$  is less than the transition point, the trajectories  $\tilde{x}^{(\Delta\lambda)}(t)$  are found to reach equilibrium, thereby allowing application of Proposition 4. Moreover, in this regime, the trajectories are in the free-flow region. When  $\Delta\lambda$  exceeds the transition point, then the trajectories are in overload, and the traffic volumes on onramps grow unbounded, which results in a higher slope in the perturbation plot in Figure 6. For  $\Delta\lambda \leq 0.8$  (corresponding to the transition point for the FIFO model), the perturbed trajectories for the FIFO and non-FIFO DNL models are identical. That is, the better robustness property of non-FIFO models can be attributed to a higher network capacity, which in turn can be attributed to flexibility in routing of traffic flow in congestion. These features are well captured by the analytical bounds computed by Proposition 3 and 4 (when an equilibrium exists) and (44) and (46) (in overload), which are shown as dashed lines in Figure 6.

Finally, the perturbed trajectories under controls derived from SO-DTA or FC-SO-DTA optimal solutions show qualitatively similar behavior, with the difference being in the locations of transition points.

## 4.2 Robustness-Performance Tradeoff under Reduced Feasible Set for DTA

The DTA formulation, whose optimal solution is used to compute controllers in Section 4.1, did not consider possible perturbations to inflow. Motivated by the observation in Section 4.1 that the network exhibits less robustness to inflow perturbations when the perturbed trajectories are in the congestion region, we suggest scaling down of the supply functions in the DTA formulations, whose optimal solution is used to set controls. Such a modification introduces more *slack*, thereby increasing the magnitude of inflow perturbations beyond which the trajectories enter the congestion region. Naturally, such a modification comes at the expense of increase in the value of optimal cost under zero perturbation. The objective in this section is to study this tradeoff.

Specifically, we replace the first inequality in (8) with

$$y_i(t) \leq s_i(x_i)(1 - \varepsilon) \tag{8'}$$

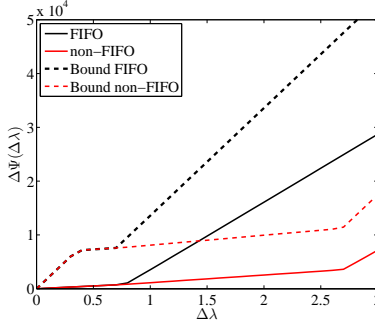


Figure 6: Comparison of the perturbation in cost due to perturbation in inflow under FIFO and non-FIFO DNL models obtained from simulations (solid lines), and the corresponding bounds from Propositions 3 and 4, (44) and (46) (dashed lines).

where  $0 \leq \varepsilon \leq 1$  is a tunable parameter. In this section, we focus on the controls computed from optimal solutions to FC-SO-DTA; the results are qualitatively similar for SO-DTA and PC-SO-DTA.

We consider again the total traffic volume cost  $\psi(x) = \sum_{i \in \mathcal{E}} x_i$  and the scenario described in Section 2.3. For a given  $\varepsilon \geq 0$ , similar to Section 4.1, we computed the control values from the optimal solution to FC-SO-DTA with initial condition  $x(0) = 0$ , and then simulated the system with several values of perturbations to inflow  $\Delta\lambda$ . The simulations were repeated for a range of values of the parameter  $\varepsilon$ . Let  $\tilde{x}^{(\varepsilon, \Delta\lambda)}(t)$  denote the perturbed trajectory. For each combination of  $\varepsilon$  and  $\Delta\lambda$ , we computed the perturbed cost:  $\Psi(\varepsilon, \Delta\lambda) := \sum_{t=0}^{25} \sum_{i \in \mathcal{E}} \tilde{x}_i^{(\varepsilon, \Delta\lambda)}(t)$ . Due to the relatively short time horizon setup of this scenario, the perturbed cost does not necessarily reflect the congestion effects in the perturbed system. Therefore, we additionally record congestion factor:  $\gamma(\varepsilon, \Delta\lambda) = \min_{j,t} \gamma_j(\tilde{x}^{(\varepsilon, \Delta\lambda)}(t))$ , where the minimum is taken over  $v \in \mathcal{V}$  and all times, and where  $\gamma_j$  is defined in (21). Clearly,  $\gamma(\varepsilon, \Delta\lambda) \leq 1$ , where equality implies that the perturbed trajectory is in free-flow all the time, whereas strict inequality implies congestion. The smaller the value of  $\gamma(\varepsilon, \Delta\lambda)$  is, the more congested some cells are.

The results are shown in Fig. 7. As expected, for every  $\Delta\lambda$ , the perturbed cost is an increasing function of  $\varepsilon$ . Concerning congestion factor,  $\gamma(\varepsilon, 0) = 1$  for all  $\varepsilon$ , as the optimal trajectory is always in free-flow, while for high  $\Delta\lambda$ , the lower  $\varepsilon$  is, the more the system is prone to congestion. At the two extremes, for  $\varepsilon = 0$  a small inflow increase yields congestion; for  $\varepsilon = 0.5$ , the perturbed solutions are in free-flow even for relatively high values of  $\Delta\lambda$ .



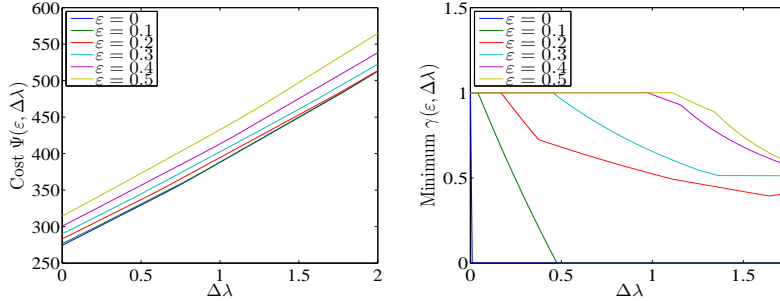


Figure 7: Impact of reduced feasible set and inflow perturbation. Left panel: cost  $\Psi(\varepsilon, \Delta\lambda)$  as a function of  $\Delta\lambda$  for different  $\varepsilon$  (colored lines). Right panel: congestion factor  $\gamma(\varepsilon, \Delta\lambda)$  as a function of  $\Delta\lambda$  for different  $\varepsilon$ .

## 5 Conclusion

We considered three variations of cell-based continuous time System Optimum Dynamic Traffic Assignment (SO-DTA) formulations that impose turning ratio constraints to varying degrees. In these formulations, similar to previous work, we consider a relaxation of realistic traffic dynamics, wherein the total inflow into and total outflow from the cells are independently upper bounded by supply and demand respectively. We also design open-loop variable speed, ramp metering and routing controllers that ensure feasibility of the optimal solutions under relaxed constraints with respect to several realistic traffic dynamics modeled by a combination of cell-based features of the Cell Transmission Model and general Dynamic Network Loading Model that includes FIFO and non-FIFO policies. We also derive bounds on perturbations in the system trajectory under the proposed open loop controllers, with respect to perturbations in initial condition and external inflow. The proposed methodologies are illustrated with extensive simulation results. These results significantly expand the known results in terms of relationship between computationally efficient SO-DTA formulations and the feasibility of their optimal solutions with respect to realistic traffic dynamics.

Future research direction includes leveraging necessary and sufficient conditions along the lines of Section 3.2 and [25, 11] to possibly speed up numerical solutions to various variants of SO-DTA. We also plan to develop distributed algorithms for solving SO-DTA and its variants, along the lines of our preliminary work in [2].

## Acknowledgements

G. Como was partially supported by the Swedish Research Council through the Junior Research Grant Information Dynamics in Large Scale Networks and the Linnaeus Excellence Center, LCCC. K. Savla was supported in part by METRANS Research Initiation Award 14-09 and NSF ECCS Grant No. 1454729.

The authors are grateful to Prof. Anders Rantzer for his many useful comments and encouragement during this research.

## References

- [1] D. Angeli. A Lyapunov approach to incremental stability properties. *IEEE Transactions on Automatic Control*, 47(3):410–421, Mar 2002.
- [2] Q. Ba, K. Savla, and G. Como. Distributed optimal equilibrium selection for traffic flow over networks. In *IEEE Conference on Decision and Control*, 2015. To appear. Available at <http://www-bcf.usc.edu/~ksavla/papers/Ba.Savla.ea.DistributedCDC15.pdf>.
- [3] E. Cascetta. *Transportation Systems Analysis*. Springer, 2009.
- [4] Y.-C. Chiu and P.B. Mirchandani. Online behavior-robust feedback information routing strategy for mass evacuation. *Intelligent Transportation Systems, IEEE Transactions on*, 9(2):264–274, 2008.
- [5] G. Como, E. Lovisari, and K. Savla. Throughput optimality and overload behavior of dynamical flow networks under monotone distributed routing. *Control of Network Systems, IEEE Transactions on*, 2(1):57–67, March 2015.
- [6] S. Coogan and M. Arcak. Dynamical properties of a compartmental model for traffic networks. In *Proceedings of the IEEE American Control Conference (ACC)*, pages 2511 – 2516, 2014.
- [7] Inc. CVX Research. CVX: Matlab software for disciplined convex programming, version 2.0. <http://cvxr.com/cvx>, August 2012.
- [8] C. F. Daganzo. The cell transmission model: A dynamic representation of highway traffic consistent with the hydrodynamic theory. *Transportation Research B: Methodological*, 28B(4):269–287, 1994.
- [9] C. F. Daganzo. The cell transmission model, part II: network traffic. *Transportation Research B: Methodological*, 29B(2):79–93, 1995.
- [10] K. Doan and S.V. Ukkusuri. On the holding-back problem in the cell transmission based dynamic traffic assignment models. *Transportation Research Part B: Methodological*, 46(9):1218 – 1238, 2012.
- [11] T.L. Friesz, J. Luque, R.L. Tobin, and B.-W. Wie. Dynamic network traffic assignment considered as a continuous time optimal control problem. *Operations Research*, 37(6):893–901, 1989.
- [12] G. Gomes and R. Horowitz. Optimal freeway ramp metering using the asymmetric cell transmission model. *Transportation Research Part C*, 14(4):244–268, 2006.

- [13] M. Grant and S. Boyd. Graph implementations for nonsmooth convex programs. In V. Blondel, S. Boyd, and H. Kimura, editors, *Recent Advances in Learning and Control*, Lecture Notes in Control and Information Sciences, pages 95–110. Springer-Verlag Limited, 2008.
- [14] A. Hegyi, B. De Schutter, and H. Hellendoorn. Model predictive control for optimal coordination of ramp metering and variable speed limits. *Transportation Research Part C*, 13(3):185 – 209, 2005.
- [15] A. Hegyi, B. De Schutter, and H. Hellendoorn. Optimal coordination of variable speed limits to suppress shock waves. *IEEE Transactions on Intelligent Transportation Systems*, 6(1):102–112, March 2005.
- [16] M. Hirsch and H.L. Smith. Competitive and cooperative systems: A mini-review. *Positive Systems. Lecture Notes in Control and Information Sciences*, 294, 2003.
- [17] I. Karafyllis and M. Papageorgiou. Global stability results for traffic networks. 2014. Submitted. Available at <http://arxiv.org/abs/1401.0496>.
- [18] M. J. Lighthill and G. B. Whitham. On kinematic waves. ii. a theory of traffic flow on long crowded roads. *Phil. Trans. R. Soc. A*, 229(1178):317–345, 1955.
- [19] E. Lovisari, G. Como, and K. Savla. Stability of monotone dynamical flow networks. In *IEEE Conference on Decision and Control*, pages 2384 – 2389, Los Angeles, CA, 2014.
- [20] D.K. Merchant and G.L. Nemhauser. A model and an algorithm for the dynamic traffic assignment problem. *Transportation Science*, 12:183–199, 1978.
- [21] D.K. Merchant and G.L. Nemhauser. Optimality conditions for a dynamic traffic assignment model. *Transportation Science*, 12:200–207, 1978.
- [22] A. Muralidharan and R. Horowitz. Optimal control of freeway networks based on the link node cell transmission model. In *Proceedings of the American Control Conference (ACC)*, pages 5769–5774, June 2012.
- [23] S. Peeta and A. K. Ziliaskopoulos. Foundations of dynamic traffic assignment: The past, the present and the future. *Networks and Spatial Economics*, 1(3-4):233–265, 2001.
- [24] I. Richards. Shockwaves on the highway. *Operations Research*, 4:42–51, 1956.
- [25] A. Seierstad and K. Sydsaeter. Sufficient conditions in optimal control theory. *International Economic Review*, pages 367–391, 1977.
- [26] A.K. Ziliaskopoulos. A linear programming model for the single destination system optimum dynamic traffic assignment problem. *Transportation science*, 34(1):37–49, 2000.

## A Proofs

### A.1 Proof of Proposition 1

(i) The choice of control parameters in (26)–(27)–(28) implies that

$$f_{ij} = \bar{R}_{ij} z_i = \bar{R}_{ij} \alpha_i d_i(x_i) = \bar{R}_{ij} \bar{d}_i(x_i), \quad i \in \mathcal{E} \setminus \mathcal{R}, j \in \mathcal{E},$$

and (by  $c_i = z_i \leq d_i(x_i)$ )

$$f_{ij} = \bar{R}_{ij} z_i = \bar{R}_{ij} \min\{d_i(x_i), c_i\} = \bar{R}_{ij} \bar{d}_i(x_i), \quad i \in \mathcal{R}, j \in \mathcal{E}.$$

Then,

$$\sum_{i \in \mathcal{E}} \bar{R}_{ij} \bar{d}_i(x_i) = \sum_{i \in \mathcal{E}} f_{ij} = y_i \leq s_j(x_j), \quad j \in \mathcal{E}, \quad (47)$$

where the inequality is implied by the supply constraint in (8). It follows from (18) that  $z_i^M = \bar{d}_i(x_i)$  for every DNL model  $M$ . This implies that

$$f_{ij}^M = \bar{R}_{ij} \bar{d}_i(x_i) = f_{ij}, \quad i, j \in \mathcal{E}, \quad (48)$$

so  $x(t)$  is the solution of (24) with initial condition  $x^0$ .

(ii) The choice of control parameters in (26)–(28) along with the additional constraint (12) of the PC-SO-DTA imply that

$$\alpha_i \bar{R}_{ij} = \frac{f_{ij}}{d_i(x_i)} \leq R_{ij}, \quad i, j \in \mathcal{E}, i \notin \mathcal{R},$$

i.e., (29) is satisfied. On the other hand, (48) can be proven in the same way as in (i).

(iii) The choice of the demand control parameters (26)–(27) along with the additional constraint (13) of the FC-SO-DTA implies, analogously to the previous case, that

$$f_{ij} = R_{ij} z_i = R_{ij} \bar{d}_i(x_i), \quad i, j \in \mathcal{E}.$$

Then,

$$\sum_{i \in \mathcal{E}} R_{ij} \bar{d}_i(x_i) = \sum_{i \in \mathcal{E}} f_{ij} = y_i \leq s_j(x_j), \quad j \in \mathcal{E},$$

where the inequality is implied by the supply constraint in (8). From this, (48) follows as in (i).  $\square$

The fact that  $x(t)$  is in free-flow under the designed control for case (i) above follows from (47) and (18). Since (47) also holds for cases (ii) and (iii), this conclusion extends to those cases too.

## A.2 Proof of Proposition 2

If  $v = \sigma_i$  is a merging junction with downstream cell  $j$ , then we immediately get that

$$(z_i^*)_{i: \tau_i=v} \in \operatorname{argmax}_{\substack{0 \leq z_i \leq d_i(x_i^*) \\ \sum_{\substack{i \in \mathcal{E}: \\ \tau_i=v}} z_i \leq s_j(x_j^*)}} \sum_{i \in \mathcal{E}: \tau_i=v} \kappa_i z_i.$$

On the other hand, if  $\tau_i$  is either an ordinary or a diverging junction, then a minimizer in (34) necessarily satisfies

$$\xi_i^* + \sum_{j \in \mathcal{E}} R_{ij} \nu_j^* = \max\{0, \kappa_i\}. \quad (49)$$

Indeed, reducing  $\xi_i \geq 0$  and  $\nu_j \geq 0$  for all  $j$  such that  $\sigma_j = \tau_i$  until  $\xi_i + \sum_{j \in \mathcal{E}} R_{ij} \nu_j = \max\{0, \kappa_i\}$  reduces the cost  $\sum_{i \in \mathcal{E}} (\xi_i d_i(x_i^*) + \nu_i s_i(x_i^*))$  without violating any of the constraints in (34). (The fact that  $\tau_i$  is either an ordinary or a diverging junction implies that such variables  $\nu_j$  appear in no constraint  $\xi_h + \sum_{j \in \mathcal{E}} R_{hj} \nu_j \geq \kappa_h$  other than for  $h = i$ .) Then, by combining (35) and (49) we get that

$$\begin{aligned} \dot{\kappa}_i &= \dot{\zeta}_i - \sum_{j \in \mathcal{E}} R_{ij} \dot{\zeta}_j \\ &= -1 + \sum_{j \in \mathcal{E}} R_{ij} + \omega \left( -\nu_i^* + \sum_{j \in \mathcal{E}} R_{ij} \nu_j^* + \xi_i^* - \sum_{j \in \mathcal{E}} R_{ij} \xi_j^* \right) \\ &\leq \omega \max\{0, \kappa_i\}, \end{aligned} \quad (50)$$

where the last step follows from the constraints  $\sum_{j \in \mathcal{E}} R_{ij} = 1$ ,  $\nu_i \geq 0$ , and  $\sum_{j \in \mathcal{E}} R_{ij} \xi_j \geq 0$ . It then follows from (50) and (36) that

$$\kappa_i(t) \geq 0, \quad t \in [0, T]. \quad (51)$$

Indeed, if  $\kappa_i(t) < 0$  for some  $t \in [0, T]$ , then (50) implies that  $\dot{\kappa}_i(t) = 0$ , hence  $\kappa_i(t') = \kappa_i(t) < 0$  for all  $t' \geq t$ , which would contradict (36). It follows that

$$z_i^* = \operatorname{argmax}_{\substack{0 \leq z_i \leq d_i(x_i^*) \\ R_{ij} z_i \leq s_j(x_j^*)}} \kappa_i z_i = \max_{\substack{0 \leq z_i \leq d_i(x_i^*) \\ R_{ij} z_i \leq s_j(x_j^*)}} z_i. \quad (52)$$

If  $\tau_i$  is an ordinary junction, then (52) reduces to (38). If  $\tau_i$  is a diverging junction, then it coincides with (39).

## A.3 Proof of Proposition 3

The proof is based on application of contraction principles, developed in our previous work [5], between system trajectories in the monotone region. Remark 1

implies that monotonicity holds everywhere for non-FIFO DNL model and in free-flow for FIFO DNL model. First note that

$$\begin{aligned}
& \frac{d}{dt} \|\tilde{x}(t) - x(t)\|_1 \\
&= \sum_{i \in \mathcal{E}} \operatorname{sgn}(\tilde{x}_i(t) - x_i(t)) (\lambda_i(t) - \tilde{\lambda}_i(t)) \\
&\quad + \sum_{i \in \mathcal{E}} \operatorname{sgn}(\tilde{x}_i(t) - x_i(t)) (g_i^M(\tilde{x}, \alpha, c, \bar{R}) - g_i^M(x, \alpha, c, \bar{R})) \\
&\leq \|\lambda(t) - \tilde{\lambda}(t)\|_1 \\
&\quad + \sum_{i \in \mathcal{E}} \operatorname{sgn}(\tilde{x}_i(t) - x_i(t)) (g_i^M(x, \alpha, c, \bar{R}) - g_i^M(\tilde{x}, \alpha, c, \bar{R})) \quad (53)
\end{aligned}$$

We first prove the result for the non-FIFO DNL model. Since (41) is satisfied globally, [5, Lemma 1] implies that the second term in the RHS of (53) is non-positive, and therefore

$$\frac{d}{dt} \|\tilde{x}(t) - x(t)\|_1 \leq \|\lambda(t) - \tilde{\lambda}(t)\|_1$$

which, upon integration, gives (42).

We consider now the FIFO model. As mentioned in the text, under FIFO DNL model, the system trajectory is not monotone in congestion. However, if  $\|\tilde{x}_0 - x_0\|_1$  and  $\|\tilde{\lambda} - \lambda\|_{1,T}$  are small enough, then the perturbed system trajectory remains in free-flow, where the system is monotone<sup>10</sup>. Thereafter, the proof for the FIFO DNL model follows along similar lines as for the non-FIFO model.

#### A.4 Proof of Proposition 4

Let  $\phi(t, x^0, \lambda)$  denote the state of the network at time  $t$  starting from initial condition  $x^0$  and under inflow  $\lambda$ . Assume that the perturbation is small enough so that the system is monotone under perturbation. Monotonicity implies that, for all  $t \in [0, T]$  and all  $i \in \mathcal{E}$ , it holds true

$$\begin{aligned}
\phi_i(t, \bar{x}^0, \bar{\lambda}) &\geq \phi_i(t, x^0, \lambda) \geq \phi_i(t, \underline{x}^0, \underline{\lambda}) \\
\phi_i(t, \bar{x}^0, \bar{\lambda}) &\geq \phi_i(t, \tilde{x}^0, \tilde{\lambda}) \geq \phi_i(t, \underline{x}^0, \underline{\lambda})
\end{aligned}$$

so

$$|\phi_i(t, x^0, \lambda) - \phi_i(t, \tilde{x}^0, \tilde{\lambda})| \leq \phi_i(t, \bar{x}^0, \bar{\lambda}) - \phi_i(t, \underline{x}^0, \underline{\lambda}) \quad (54)$$

In addition, [5, Lemma 1] implies that

$$\|\phi(t, x, \lambda) - \phi(t, y, \lambda)\|_1 \leq \|x - y\|_1, \quad \forall t \in [0, T] \quad (55)$$

<sup>10</sup>This is ensured by the properties of monotone controlled systems [1], for which the trajectory is continuous in the external inflows (seen as inputs to the system).

Therefore,

$$\begin{aligned}
& \|\phi(t, x^0, \lambda) - \phi(t, \tilde{x}^0, \tilde{\lambda})\|_1 \\
& \leq \|\phi(t, \bar{x}^0, \bar{\lambda}) - \phi(t, \underline{x}^0, \underline{\lambda})\|_1 \\
& \leq \|\phi(t, \bar{x}^0, \bar{\lambda}) - \phi(t, \bar{x}^0, \underline{\lambda})\|_1 + \|\phi(t, \bar{x}^0, \underline{\lambda}) - \phi(t, \underline{x}^0, \underline{\lambda})\|_1 \\
& \leq \|\phi(t, \bar{x}^0, \bar{\lambda}) - x^{\text{eq}}(\bar{\lambda})\|_1 + \|x^{\text{eq}}(\bar{\lambda}) - x^{\text{eq}}(\underline{\lambda})\|_1 \\
& \quad + \|x^{\text{eq}}(\underline{\lambda}) - \phi(t, \bar{x}^0, \underline{\lambda})\|_1 + \|\phi(t, \bar{x}^0, \underline{\lambda}) - \phi(t, \underline{x}^0, \underline{\lambda})\|_1 \\
& \leq \|\bar{x}^0 - x^{\text{eq}}(\bar{\lambda})\|_1 + \|x^{\text{eq}}(\bar{\lambda}) - x^{\text{eq}}(\underline{\lambda})\|_1 + \|x^{\text{eq}}(\underline{\lambda}) - \bar{x}^0\|_1 + \|\bar{x}^0 - \underline{x}^0\|_1
\end{aligned} \tag{56}$$

where the first inequality follows from (54), the second and third by triangle inequality, and the fourth by (55). Also, by exchanging the two terms of the difference after the first inequality in (56), we have

$$\begin{aligned}
\|\phi(t, x^0, \lambda) - \phi(t, \tilde{x}^0, \tilde{\lambda})\|_1 & \leq \|\underline{x}^0 - x^{\text{eq}}(\underline{\lambda})\|_1 + \|x^{\text{eq}}(\underline{\lambda}) - x^{\text{eq}}(\bar{\lambda})\|_1 \\
& \quad + \|x^{\text{eq}}(\bar{\lambda}) - \underline{x}^0\|_1 + \|\underline{x}^0 - \bar{x}^0\|_1.
\end{aligned} \tag{57}$$

The result follows by combining (56) and (57).